ELSEVIER

Biochimica et Biophysica Acta 1463 (2000) 151–161

BIOCHIMICA ET BIOPHYSICA ACTA
BBA

www.elsevier.com/locate/bba

# Structural and orientational information of the membrane embedded M13 coat protein by $^{13}$C-MAS NMR spectroscopy

Clemens Glaubitz *, Gerhard Gröbner, Anthony Watts

*Biomembrane Structure Unit, Department of Biochemistry, University of Oxford, South Parks Road, Oxford OX1 3QU, UK*

Received 12 July 1999; received in revised form 28 September 1999; accepted 28 September 1999

**Abstract**

Oriented and unoriented M13 coat protein, incorporated into dimyristoyl phosphatidylcholine bilayers, has been studied by $^{13}$C-magic angle spinning nuclear magnetic resonance (MAS NMR) spectroscopy. Rotational resonance experiments provided two distance constraints between C$\alpha$ and C=O positions of the labelled residues Val-29/Val-30 ($0.4 \pm 0.5$nm) and Val-29/Val-31 ($0.45 \pm 0.5$nm) in its hydrophobic domain. The derived dihedral angles ($\Phi$, $\Psi$) for Val-30 revealed a local $\alpha$-helical conformation. $^{13}$C-CP-MAS experiments on uniformly aligned samples (MAOSS experiments) using the $^{13}$C=O labelled site of Val-30 allowed the determination of the helix tilt ($20° \pm 10°$) in the membrane. It is shown that one uniform MAS high-resolution solid state NMR approach can be used to obtain structural and orientational data. 

*Keywords:* Solid-state NMR; MAS; MAOSS; Oriented membrane; Peptide; M13 coat protein; Lipid

## 1. Introduction

M13 coat protein (5240 Da, 50 residues) has been studied extensively due to the intriguing requirement that it has to adapt to three different environments, in the bacteriophage as a coat protein, in the inner *Escherichia coli* plasma membrane as membrane protein and after synthesis across the cytoplasm prior membrane insertion. The protein sequence (Fig. 1) can be divided into three regions; an acidic domain of 20 residues, a hydrophobic domain of 19 and a basic domain of 11 amino acids [1]. The hydrophobic region is believed to span the cytoplasmic membrane of the target cell [2].

X-ray diffraction has shown a complete $\alpha$-helical secondary structure of M13 in the intact phage particle, with the overall helix axis approximately parallel to the filamental axis [3]. A disordered helical structure for residues 40–45 of the closely related fd-coat protein has been found by solid-state nuclear magnetic resonance (NMR) [4], which agrees well with diffraction studies in which a slightly twisted helix is observed [5]. The membrane-bound form of the coat protein has been studied extensively resulting in the construction of several structural models. The coat protein dissolved in detergent micelles and bilayers has been described as an arrangement of dimers with a large fraction of $\alpha$-helix and $\beta$-sheet [6,7] but also as a predominantly $\alpha$-helical monomer

Abbreviations: NMR, nuclear magnetic resonance; MAS, magic angle spinning; MAOSS, magic angle oriented sample spinning; DMPC, dimyristoyl phosphatidylcholine

* Corresponding author. Fax: +44-1865-275234;
E-mail: glaubitz@bioch.ox.ac.uk

0005-2736/00/$ – see front matter 
PII: S0005-2736(99)00195-9

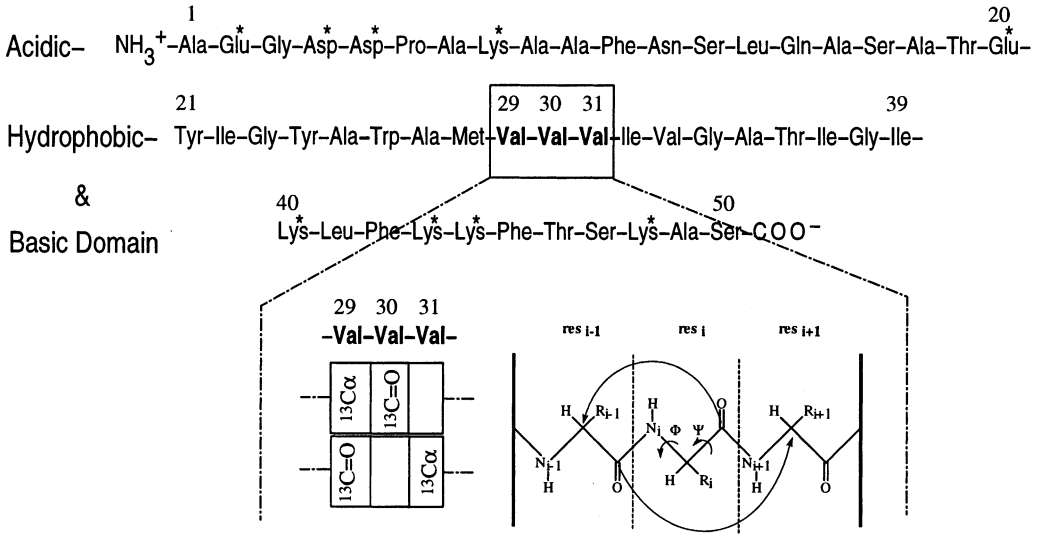


Fig. 1. Amino acid sequence of major coat protein M13. Three domains are found: an acidic N-terminus of 20 residues, a hydrophobic domain 19 residues and a basic C-terminus of 11 residues. Charged, polar amino acids are labelled with *. Two samples were prepared, each with a pair of $^{13}C\alpha$-$^{13}C=O$ labels in Val-29/Val-30 and Val-29/Val-31, as indicated below the sequence. The distances [α29,30] and [29,α31] define the dihedral angles $\Phi$ and $\Psi$ of Val-30.

[9], depending upon the isolation and purification procedures used [9]. A form in which the protein adopts a β-sheet structure has also been found [10], but only the α-helical monomeric form is used in the present study.

The membrane bound form of the closely related fd-coat protein has been characterized by combining two-dimensional liquid-state and solid-state NMR suggesting a long hydrophobic helix crossing the membrane and a shorter amphipathic helix which lies in the plane of the bilayer [8]. Dynamic studies on fd as well as M13 coat protein revealed that the hydrophobic, transmembrane domain is motionally restricted on the relevant NMR time-scales, while the amphipathic helix is less restricted [11–14].

Here, magic angle spinning (MAS) NMR is used to determine local conformation and orientation of the hydrophobic core of M13 coat protein in the lipid bilayer.

## 2. Materials and methods

### 2.1. Rotational resonance NMR

Rotational resonance NMR spectroscopy can be used to determine internuclear distances in solids [15]. It is based on the measurement of the homonuclear dipole-dipole interaction, which is proportional to $r_{IS}^{-3}$, where $r_{IS}$ is the internuclear distance:

$$b_{IS} = -\frac{\mu_0}{4\pi}\left(\frac{\gamma_I \gamma_S \hbar}{r_{IS}^3}\right) \quad (1)$$

Although the direct dipole-dipole coupling is attenuated during MAS, it reappears when the sample spinning rate $\omega_r$ is adjusted to satisfy the condition $\Delta\omega_{iso} = n\omega_r$, where $\Delta\omega_{iso}$ is the isotropic chemical shift difference and $n$ a small integer (1,2,3 etc.). Reintroducing the dipolar coupling leads to an enhancement of Zeeman magnetization exchange, which can easily be measured [15–17].

### 2.2. MAS NMR on oriented systems

While rotational resonance experiments on unoriented samples provide detailed and precise information about local conformation, NMR experiments on oriented membranes provide additional orientation constraints. It has been shown that MAS applied to ordered systems, such as oriented bacteriorhodopsin, is a feasible approach to study orientations of molecular groups in membrane proteins [18,19]. Uniformly aligned samples on glass disks can be fixed in a MAS rotor so that the sample director reference frame and the rotor frame are identical. If the spinning rate $\omega_r$ is smaller than the chemical shift aniso-

tropy, spinning sidebands will appear equally spaced by $\omega_r$ about the isotropic chemical shift resonance line. Each sideband intensity $I_N$ is a function of orientation and principal elements of the chemical shift tensor [20–22]. Knowledge of the protein secondary structure permits the definition of an intermediate, molecular-fixed reference frame, which provides a relationship between the chemical shift tensor orientation and the molecular orientation with respect to the membrane plane. Protein orientation and position within the anisotropic membrane environment can so be determined.

### 2.3. Sample preparation

#### 2.3.1. Materials

L-α-Dimyristoyl phosphatidylcholine (DMPC) was obtained from Sigma (UK) and used without further purification. L-α-DMPC-$d_{67}$ was obtained from Avanti Polar Lipids (USA). Two doubly $^{13}C$ labelled samples of M13 coat protein were synthesized using standard solid-phase FMOC chemistry (NSR Centre, Nijmegen, The Netherlands). Asp-5 was replaced by Asn. The labelled positions in the first sample (M13[α29,30]) were (2-$^{13}C$) in Val-29 and (1-$^{13}C$) in Val-30 and in the second (M13[29,α31]) (1-$^{13}C$) in Val-29 and (2-$^{13}C$) in Val-31, as illustrated in Fig. 1. The purity of the synthesized peptide was found to be over 90% as measured by HPLC and mass spectroscopy.

#### 2.3.2. Sample preparation

The protocol for incorporation of M13 coat protein into DMPC bilayers at a lipid to protein molar ratio of 30:1 was adapted from methods described before [23]. The peptide was dissolved in TFA (10 mg peptide in 200 μl TFA) to break up any aggregates. After the removal of TFA under a stream of nitrogen, 5 ml of TFE were added to resuspend the protein film and evaporated to remove any traces of acidic TFA. The film was then dissolved in 0.5 ml of TFE and subsequently reconstitution buffer (10 mM $NaH_2PO_4$, 0.2 mM EDTA, 140 mM NaCl, 150 mM sodium cholate at pH 7.8) was added in 0.5 ml aliquots under vortexing to obtain a clear solution of 8 ml volume in total. The desired amount of DMPC lipid was solubilized in 3 ml of reconstitution buffer, added to the M13 solution and vigorously mixed. After incubation (30 min, 30°C) the solution was filled in an appropriate dialysis tube and subsequently dialyzed (2 weeks, 4°C) against 1 l of dialysis buffer (reconstitution buffer without cholate) where 500 ml buffer were replaced every 24 h. After complete reconstitution, the vesicles were pelleted, resuspended in dialysis buffer and layered on a linear sucrose gradient (0–40% w/w). Centrifugation (12 h, 4°C; $90\,000 \times g$) in a SW28 swinging bucket rotor (Beckman, USA) produced a single layer at 22% w/w sucrose indicating a homogeneously reconstituted sample. The layer was recovered and the sucrose removed by several washing steps in reconstitution buffer. The lipid-protein molar ratio was determined by standard phosphate and protein assays. Incorporation of the protein in an α-helical form [23] was checked by CD-measurements (Jasco, USA). Trials to obtain pure β-sheet conformation were not successful.

For rotational resonance NMR experiments, sample pellets (40 mg lipid and protein) were centrifuged into a Bruker 4 mm MAS rotor after some freeze-thaw cycles. Oriented M13 samples for magic angle oriented sample spinning (MAOSS) experiments were prepared by covering precisely cut glass disks (5.4 mm diameter, 0.1 mm thickness, Marienfelde GmbH) with peptide/lipid complex (0.3 mg in 25 μl diluted buffer solution). To decrease the lipid background signal in CP-MAS experiments, DMPC-$d_{67}$ was used for reconstitution. Some bulk water was allowed to evaporate (24 h at 4°C). Macroscopic order in the sample was pre-checked using polarized light microscopy. Disks (80) were stacked on top of each other and rehydrated in a sealed container (93% relative humidity using saturated $NH_4H_2PO_4$ solution at 30°C [24]) over 5 days. Finally, the disks were transferred into Bruker 7 mm MAS rotors. KelF inserts were placed on top of the disks in the MAS rotor.

Sample orientation and stability was monitored by static $^{31}P$ NMR before and after the MAS experiments. No changes in the spectral lineshape were detected. The mosaic spread $\Delta\beta$ was typically between $\pm 10$ and $\pm 20°$.

### 2.4. NMR experiments

All NMR experiments were performed at 100.63

MHz for $^{13}C$ and 400.13 for $^{1}H$ on Bruker MSL-400 and Avance-400 spectrometers. Rotational resonance data were acquired using a double resonance Bruker 4 mm probe. Typical 90° pulse lengths were 4 and 6 μs for $^{13}C$ and $^{1}H$, respectively. Cross polarization was accomplished using a ramped-amplitude contact pulse sequence. A CP contact time of 2.5 ms, a repetition delay time of 2.0 s and a decoupling power of 60 kHz were applied. The carbonyl resonance was selectively inverted by applying a DANTE sequence [25] followed by the free evolution of the spin system for a variable mixing time $\tau$ (0–40 ms) under strong proton decoupling. Although many attempts were undertaken to observe magnetization exchange trajectories at $n=1$ rotational resonance condition which corresponds at the used field of 9.8 T to a spinning rate of $\omega_r = 11146.5$ Hz, it was not possible to stabilize the rotor at this speed within a sufficient rotor speed accuracy over a necessary period of time. Experiments at higher orders of resonance however, were possible without problems. The spinning rate was controlled to within $\pm 2$ Hz. Temperature was regulated by a Bruker BT3000 temperature control unit. Experiments were performed at temperatures between 243 and 310 K. CP-MAOSS experiments were performed on a Bruker 7 mm double resonance probe at 243 K. Sample stability was checked before and after sample spinning by static $^{1}H$ and $^{31}P$ NMR. The chemical shielding tensors were characterized by sideband analysis from low speed MAS spectra of unoriented M13/DMPC-$d_{67}$ complex. For both $^{13}C\alpha$, $\sigma_{iso} = 64.3$ ppm, $\delta = -10.70$ ppm and $\eta = 0.3$ were found. The $^{13}C=O$ tensors are characterized by $\sigma_{iso} = 175.1$ ppm, $\delta = -76.50$ ppm and $\eta = 0.96$. Spectra were analyzed using Felix (Biosym). Numerical simulations were performed on Silicon Graphics INDY 5600 workstations as described before [19]. Intensities of the $^{13}C=O$ and $^{13}C\alpha$ resonances were determined by integration. A natural abundance correction was performed by analyzing the spectrum of unlabelled M13 coat protein.

## 3. Results

### 3.1. Determination of internuclear distances

A $^{13}C$-CP-MAS spectrum of M13[α29,30] in DMPC bilayers is shown in Fig. 2. The resonances arising from (2-$^{13}C$)-Val29 and (1-$^{13}C$)-Val30 are labelled. Magnetization exchange experiments were performed at various temperatures in order to evaluate the effect of molecular motions. If a labelled molecule undergoes fast anisotropic reorientations, the bipolar coupling would be projected onto the long axis and analyzing rotational resonance effects would yield an incorrect distance. Here, no significant difference in the magnetization exchange rate at temperatures between 243 and 293 K was found, which corresponds to the NMR dynamic studies on M13 suggesting that the hydrophobic domain (res. 21–39) is motionally restricted on the NMR time scale [11–14]. Zeeman magnetization exchange trajectories at $n=2$ resonance condition and at $T=4$°C for the samples M13[α29,30] and M13[29,α31] are shown in Fig. 3. The difference magnetization $\langle I_z - S_z \rangle$ of both resonances is plotted over the mixing time. A significant signal decay is observed for both samples over a mixing time of $\tau = 40$ ms, which can be analyzed following a formalism published previously [26]. However, at higher orders of rotational resonance, not only the chemical shift tensors principal elements but also their orientation influence the magnetization exchange trajectory. A careful data analysis is therefore necessary in order to avoid assumptions about a certain molecular conformation.

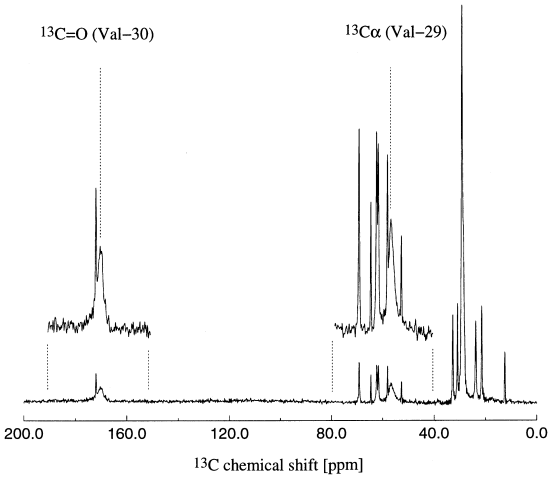


Fig. 2. $^{13}C$-CP-MAS NMR spectrum at 100.63 MHz of M13[α29,30], reconstituted in DMPC bilayers (L/P = 30; 10 mg peptide, 40 mg lipid) at 25°C and $\omega_r = 11\,000$ Hz.

Five Euler angles describe the orientation of both chemical shielding tensors with respect to each other

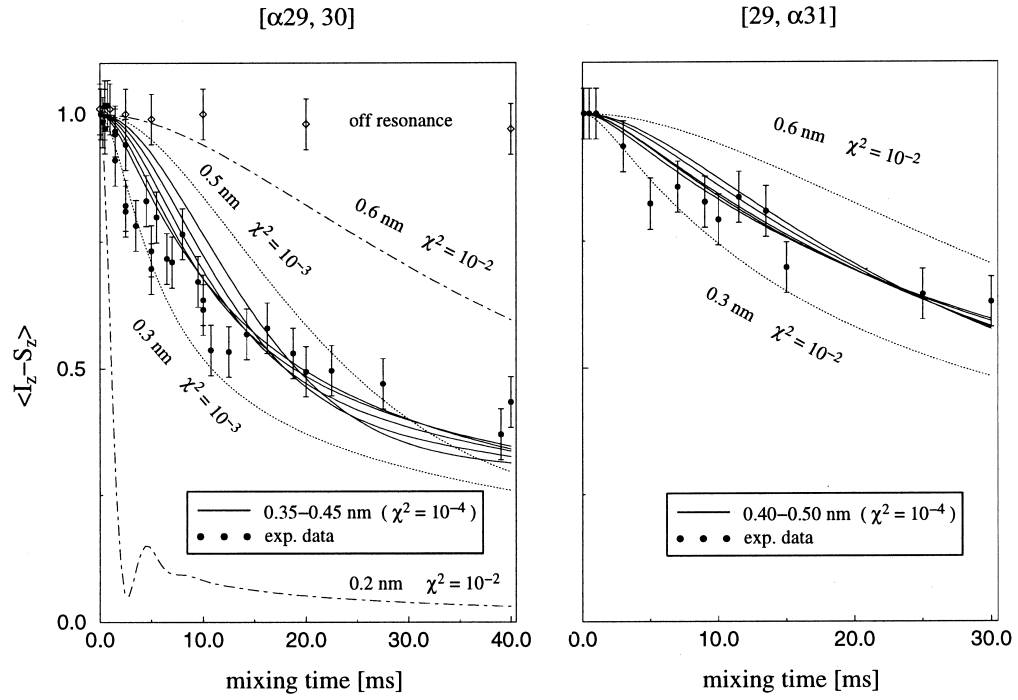


Fig. 3. Magnetization exchange curves for M13[α29,30] and M13[29,α31] at n = 2 rotational resonance condition. The difference magnetization $\langle I_z - S_z \rangle$ of both spin pairs is plotted over the mixing time. All experimental points are plotted with error bars. An off resonance exchange curve for M13[α29,30] does not show any decay, while on resonance, a magnetization exchange is observed. Data were analyzed by fitting the relative tensor orientations and $T_2^{ZQ}$ within certain limits and for a set of fixed distances to the exchange curves (see text for details). This procedure yields a distance of 0.4 ± 0.05 nm for [α29,30] and 0.45 ± 0.05 nm for [29,α31] without making any assumptions about relative shielding tensor orientations.

and with respect to the molecular frame MF. Since the chemical shift anisotropy of Cα is much smaller and nearly symmetrical when compared to C = O, the molecular frame MF can be chosen to be identical with the principal axis system of Cα and with the dipolar coupling tensor. This leaves five unknown in the data analysis; three Euler angles, the dipolar coupling and $T_2^{ZQ}$ (a phenomenological relaxation parameter). A lower limit of 2 ms for the latter could be estimated from the linewidth of $^{13}$Cα and $^{13}$C = O [16]. The experimental exchange curves were now fitted by stepping the distance $r_{IS}$ from 0.2 to 0.6 nm in 0.01 nm steps while searching for the best fit for each step by varying the C = O tensor orientation and $T_2^{ZQ}$. This was done by the Monte Carlo method and by combining the rotational resonance simulation algorithm with the CERN minimization library MINUIT [27].

The $\chi^2$ value for each solution was used to compare fitting results for different distances with each other. The result is plotted over the experimental data in Fig. 3. It is shown that a best fit with $\chi^2 \simeq 10^{-4}$ can be obtained for distances of $r_{IS}$ = 0.4 ± 0.05 nm for M13[α29,30] and $r_{IS}$ = 0.45 ± 0.05 nm for M13[29,α31]. This approach allows $n = 2$ exchange curves to be analyzed without prior knowledge of a molecular structure, which is however reflected in a larger error on the distances. Typical fitting results for $T_2^{ZQ}$ were between 3 and 8 ms, which is in the range of values used throughout the literature for comparable systems [28]. The effect of inhomogeneous linebroadening to the rotational resonance analysis has also been evaluated, but it was found to be negligible within the determined error limits [29].

The obtained distance constraints can be used to calculate dihedral angles $\Phi$ and $\Psi$ for Val-30, as indicated in Fig. 1 [30]. The set of all possible angle combinations was generated using the software Discover3/InsightII (Biosym, San Diego, CA, USA) and

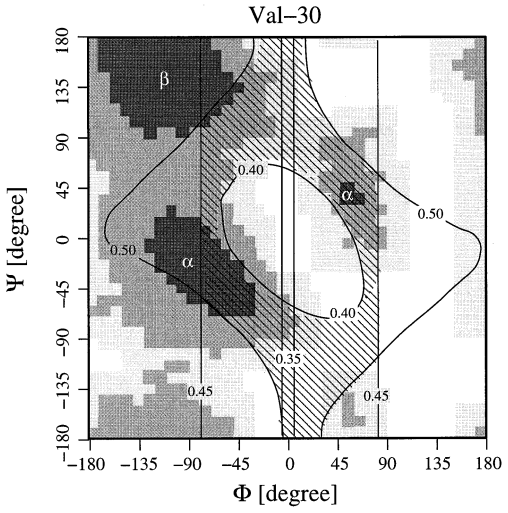


Fig. 4. [$\Phi-\Psi$]-contour map for Val-30: The NMR determined distance constraints M13[α29,30] = 0.35 to 0.45 nm and M13[29,α31] = 0.4 to 0.5 nm define an area of allowed $\Phi/\Psi$ angles (shaded), which covers the most favorable region for α-helical conformation (α), but excludes β-sheet structures (β).

is plotted over a Ramachandran plot created by ProCheck (Fig. 4). The shaded region defines the angle subset, which would agree with the obtained NMR distance constraints. It can be seen that the most favored region α, which corresponds to an α-helical structure, agrees well with the NMR distance constraints, while a β-sheet conformation can be reliably excluded.

### 3.2. Helix tilt angle determination

The orientation of the C=O shielding tensor for all amino acids is intimately related to the amide plane and the direction of the C=O bond [31–33]. The most shielded component $\sigma_{33}$ in extended, sheet and helical conformation lies along the director of the peptide plane (Fig. 5). The component that lies close to the C=O bond is $\sigma_{22}$. The least shielded component also lies in the amide plane and is perpendicular to the C=O bond [34] and is an excellent probe for protein structures, especially for determining the orientation of membrane protein subunits. Since the rotational resonance experiments reveal an α-helical secondary structure, a molecular reference frame MF can now be defined with a $z$-axis $Z_M$ as the helix long axis. The orientation of the $^{13}C=O$ shielding tensor in Val-30 can so be described within the protein allowing the helix orientation within the membrane plane to be determined. The necessary reference frame rotations from the chemical shift tensors principal axes system PAS to the molecular

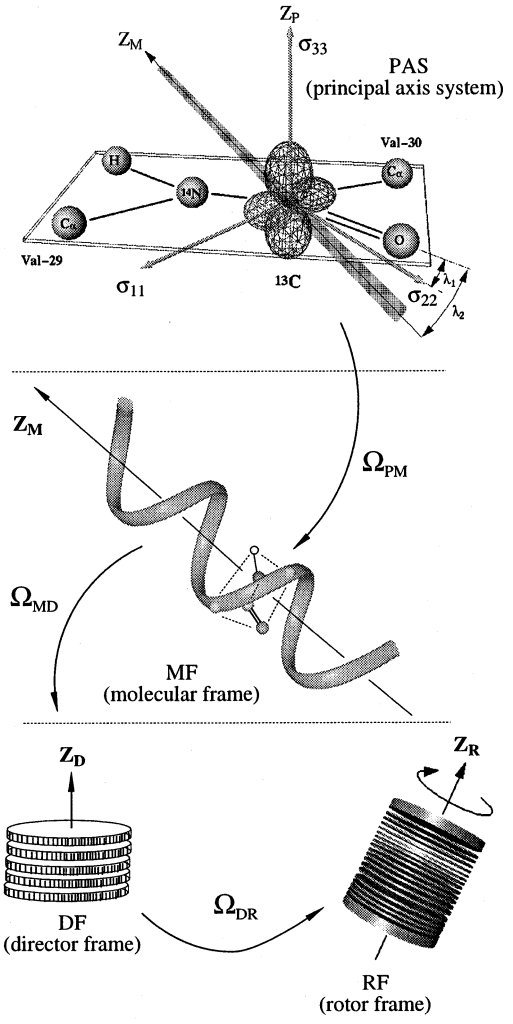


Fig. 5. Reference frames for a carbonyl labelled site in a protein backbone: Two Euler angles are needed to describe the rotations about $\sigma_{33}$ ($\alpha_{PM} = -80$–$-90°$) and $\sigma_{22}$ ($\beta_{PM} = 85$–$90°$), which relate the principal axis system of the $^{13}C=O$ shielding tensor to the peptide plane and so to the molecular reference frame. $\lambda_1$ and $\lambda_2$ are the angles between the C=O bond vector and $\sigma_{22}$ and $Z_M$. The orientation of the helix with respect to the membrane normal is given by the tilt angle $\beta_{MD}$ while an additional rotation about $Z_M$ by $\alpha_{MD}$ fixes the position of the $^{13}C=O$ label within the helix. The transformation form the director frame into the MAS rotor frame requires averaging over $\alpha_{DR}$ from 0 to 360° to account for the two-dimensional distribution in the membrane, while remaining orientational disorder $\Delta\beta$ is included by $\beta_{DR} = \pm\Delta\beta$.

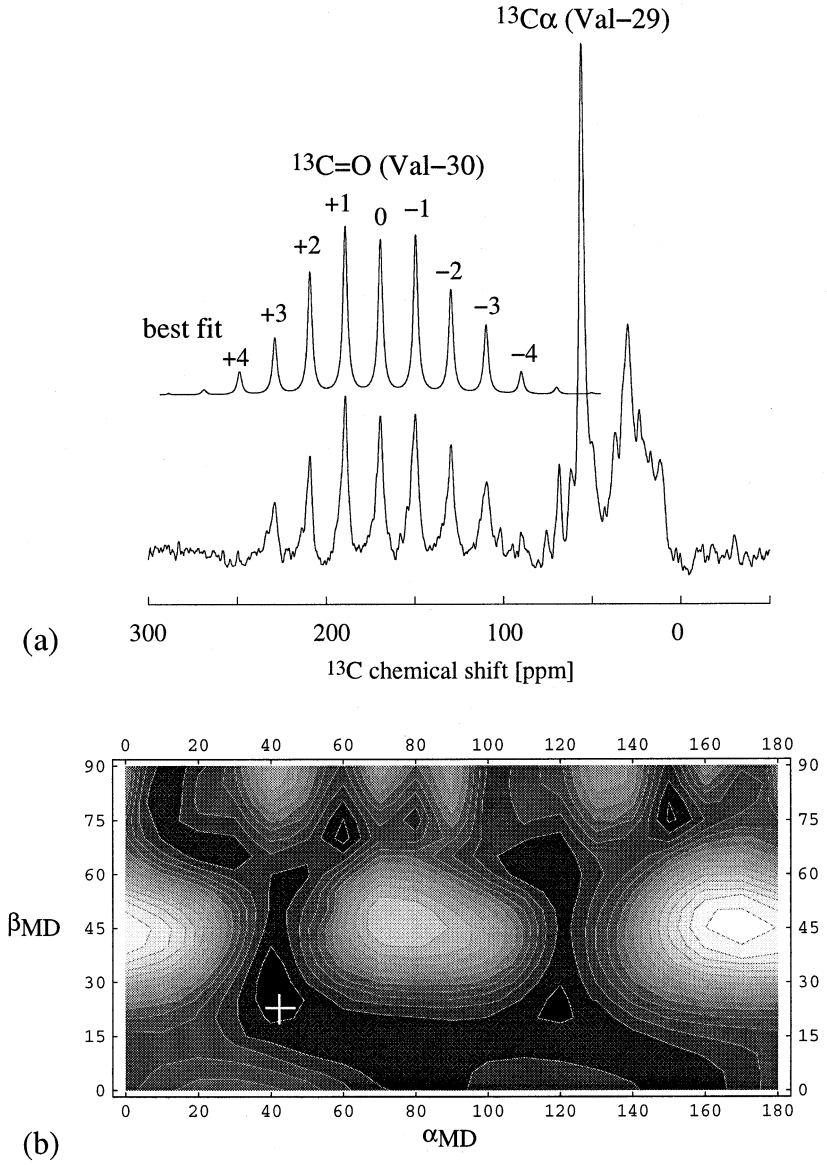


Fig. 6. $^{13}$C-CP-MAOSS NMR spectrum of M13 in DMPC-$d_{67}$ (L/P = 30) at $\omega_r = 2000$ Hz and $T = 243$ K (a). The best-fit search (b) for the spinning sideband pattern of $^{13}C=O$ in Val-29 was carried out in the $\alpha_{MD}/\beta_{MD}$ parameter space for different mosaic spread values $\Delta\beta$, which revealed a average helix tilt of 20°.

frame MF, from their to the director frame DF and finally into the MAS rotor frame RF are indicated in Fig. 5 and explained below.

### 3.3. PAS to MF

The angle $\lambda_1$, that $\sigma_{22}$ makes with the C=O bond, has been determined to be between 0 and 30° from single crystal studies and solid state NMR experiments on various model compounds [31–33]. The angle $\lambda_2$ in Fig. 5 relates the orientation of the C=O bond vector with respect to the molecular long axis $Z_M$, which is close to being colinear to the N-H bond vector. The angle between the C=O and N-H bond in an ideal peptide plane is 3.7° [35]. With these data, Euler angles $\alpha_{PM}$, $\beta_{PM}$, which relate the shielding tensor to the molecular frame MF have been determined to be between 85 and 90° for $\beta_{PM}$

and −80° and −90° for $\alpha_{PM}$. The angle $\gamma_{PM}$ can be set to 0° since it describes the same rotation as $\alpha_{MD}$.

### 3.4. MF to DF

The parameter of interest is the helix tilt angle $\beta_{MD}$. However, a second angle $\alpha_{MD}$ is necessary which describes rotation about the helix axis $Z_M$ and which fixes the position of the $^{13}C=O$ label within the helix. If the helix is parallel to the membrane director $Z_D$, no $\alpha_{MD}$ dependence of the MAOSS spectrum would be observed, while in case of rotation about $Z_M$, all values $\alpha_{MD}$ would have the same probability. As before, the angle $\gamma_{MD}$ can be set to 0° since it describes the same rotation as $\alpha_{DR}$.

### 3.5. DF to RF

The sample director frame is identical with the MAS rotor frame (Fig. 5). However, averaging over $\alpha_{DR}$ and $\gamma_{DR}$ are necessary to account for the two-dimensional distribution within the oriented samples and for unsynchronized data sampling. Additionally, a certain distribution $\Delta\beta$ of the local director axis $Z_D$ with respect to the rotor axis $Z_R$ caused by some remaining disorder is best described by a Gaussian probability distribution about $\beta_{DR}=0°$ with a weighting factor of $\sin\beta_{DR}$ [19,36]:

$$p_{DR}(\beta_{DR}) = M \int_0^{\beta_{DR}} \exp\left[-\frac{1}{2}\left(\frac{\beta}{\Delta\beta}\right)^2\right] \sin\beta \,\mathrm{d}\beta \tag{2}$$

where $M$ is an normalization constant.

The intensity of a MAS sideband $I_N$, taking disorder and the two-dimensional distribution in a membrane into account, is now formally described as:

$$I_N(\alpha_{PM},\ \beta_{PM},\ \alpha_{MD},\ \beta_{MD},\ \Delta\beta) =$$

$$K \int_0^{2\pi} \mathrm{d}\alpha_{DR} \int_0^{2\pi} \mathrm{d}\gamma_{DR} \int_{-\Delta\beta}^{+\Delta\beta} \mathrm{d}\beta_{DR} \tag{3}$$

$$\times p_{DR}(\beta_{DR}) \times I_N(\Omega_{PR}) \tag{4}$$

with $K$ being an integration constant. All subsequent rotations are well described by Wigner rotation matrices:

$$D_{qi}^{(2)}(\Omega_{PR}) =$$

$$\sum_{j=-2}^{+2} \sum_{k=-2}^{+2} D_{qk}^{(2)}(\Omega_{PM})\, D_{kj}^{(2)}(\Omega_{MD}) D_{ji}^{(2)}(\Omega_{DR}) \tag{5}$$

Explicit expressions for $I_N$ can be found elsewhere [20,37]. A MAS spectrum of oriented M13[α29,30] is shown in Fig. 6a. The spectrum was acquired at 2000 Hz spinning rate at a temperature of 243 K. The isotropic chemical shift of the carbonyl signal of Val-30 is surrounded by a set of spinning sidebands. The best fit was found by scanning the $\alpha_{MD}/\beta_{MD}$ parameter space for different degrees of disorder ($\Delta\beta$) as shown in the $\chi^2$-plot in Fig. 6b. It revealed a helix tilt angle $\beta_{MD}=20°$ with $\alpha_{MD}=42°$ and a mosaic spread of 25°. It is important to analyze potential error sources in order to estimate the accuracy of the obtained peptide tilt angle. The largest error contributions arise from uncertainties in determining the orientation and size of the $^{13}C=O$ shielding tensor. Their influence has been evaluated by varying systematically the values while fitting the experimental spectrum. An error range of ±10° for $\beta_{MD}$ could so be estimated.

The $^{13}C$ natural abundance of 1%, another potential error source, creates in this 50 residue protein a spectral background of ca. 33%. However, the isotropic chemical shift of peptide backbone carbonyls is distributed over a range of 172–177 ppm, so only a broadening in the baseline of the MAS spinning sidebands would be expected. The natural abundance adds to the experimental error but does not change the result significantly. The same applies to the effect the different degrees of disorder would have. The fitting procedure would return the same result but with larger uncertainty.

The measurements of carbonyl $^{13}C$ chemical shift tensors in peptide planes could be complicated by direct bipolar interactions to the adjacent $^{14}N$ nucleus [38,39]. Nitrogen-14 with a natural abundance of 99.63% has a spin $I=1$ and is thus a quadrupolar nucleus. It has been shown that MAS fails to completely eliminate the coupling between $^{13}C$ and $^{14}N$ and a residual bipolar coupling $b_{res}$ can be observed in lower magnetic fields [33,39,40] for which an ex-

pression has been derived by Olivieri [41]:

$$b_{res} = -\frac{3}{20}\frac{b_{IS}\chi}{\omega_I}$$

$$(3\cos^2\beta_{EFG} - 1 + \eta\sin^2\beta_{EFG}\cos 2\alpha_{EFG}) \qquad (6)$$

where $b_{IS}$ is the dipolar coupling between both nuclei, $\omega_I$ is the Larmor frequency of $^{14}N$ and $\chi$ is the quadrupolar coupling constant, $\chi = e^2qQ/h$. The angles $\alpha_{EFG}$ and $\beta_{EFG}$ describe the orientation of the bipolar coupling tensor with respect to the electric field gradient tensor frame. Splittings have been actually observed in fields of up to 4.6 T [33,40] but the expression above shows that the residual dipolar coupling decreases with increasing field strength (Larmor frequency). It can be concluded, that the $^{14}N$-$^{13}C$ coupling has a negligible influence on $^{13}C$ NMR MAS spectra of amides for $B_0 \geq 4.7$ T [33]. Summarizing, it can be stated that the tilt of the protein region around residues 29–31 is found to be $\beta_{MD} = 20 \pm 10°$.

## 4. Discussion

Various studies on M13 and similar coat proteins in lipid bilayers, detergents and organic solvents generally agree with the view that M13 coat protein is largely α-helical under conditions similar to the in vivo state in the cell plasma membrane, but our results represent a direct proof of α-helical conformation for residues 29–31 while the protein is in the lipid bilayer [8,42–45]. Since the apolar domain of M13 coat protein has the correct length to span the hydrophobic core of the *E. coli* plasma membrane as an α-helix, an orientation parallel to the membrane normal has been suggested, which was proven by static solid state NMR experiments on oriented membranes [8]. It has been shown from the $^{15}N$ resonances of Leu-14, Tyr-24, Tyr-32 and Leu-41 of the closely related fd-coat protein, that the hydrophobic domain is approximately parallel and the acidic (N-terminal) domain approximately perpendicular to the membrane normal [8,46]. The result of a slight helix tilt with respect to the membrane normal confirms and extends the model based on these findings. It does not contradict previous work, since our angular resolution for orientations about the membrane normal is higher than for the methods (FTIR and static NMR) used before [45,46]: The anisotropic chemical shift $\omega_{CS}$ of $^{13}C$ or $^{15}N$ labelled sites in proteins in oriented membranes, with the membrane normal parallel to $B_0$ observed by static NMR, is directly related to the shielding tensor orientation and so to the helix orientation with respect to the membrane:

$$\omega_{CS} \propto 3\cos^2\beta_{PD} - 1 - \eta\sin^2\beta_{PD}\cos 2\alpha_{PD} \qquad (7)$$

The highest angular resolution is achieved around $\beta_{PD} = 54.7°$, while the spectral response close to $\beta_{PD} = 0°$ is less sensitive. However, in a MAOSS experiment, the sample director is tilted to $\theta = 54.7°$, which increases the sensitivity around $\beta_{PD} = 0°$ remarkably. For the lower spectral resolution due to complex lineshapes is accounted for by sample spinning which is refocusing all spectral intensity in narrow MAS sidebands.

Many known membrane-spanning α-helices tend to be tilted at angles between 5° and 40° with a mean of 20° [47]. It has also been suggested [5] that a tilt of the M13 coat protein in the membrane would actually allow an easier insertion into the virion, in which the protein is tilted as well. Interestingly, the helix tilt angle of $20 \pm 10°$ with respect to the membrane coincides with the tilt of 20° of residues 28–32 in the bacteriophage with respect to the phage long axis, as measured by static solid state NMR [48], which would support the model suggested by Marvin [5]. The relatively large mosaic spread $\Delta\beta$ of $\pm 15°$ obtained for the protein could arise partially from conformational heterogeneity. The loop-hinge region of the protein (residues 17–26) undergoes a large structural change during phage assembly, as the in-plane helix tilts nearly perpendicular to the hydrophobic helix [12]. It has been suggested that slightly different conformations might be tolerated in the membrane bound form, which could cause a certain distribution of the tilt angle of the transmembrane helix around residue 30 [49].

The aim of this study is to show that MAS NMR spectroscopy on unoriented and oriented samples can provide valuable information about local conformational and orientational details of selectively labelled membrane proteins. The applicability of the MAOSS approach for measuring the orientation of α-helical peptides has been demonstrated by using the chemical shift anisotropy of the carbonyl group. It has

been shown by using a MAS high-resolution solid state NMR approach, that the transmembrane domain of M13 coat protein is α-helical and slightly tilted with respect to the membrane normal, which agrees with published data and extends the accepted model [5].

## Acknowledgements

Christina M. Szabo and Lori Sanders, University of Illinois are acknowledged for providing information about $^{13}C=O$ shielding tensor orientation. Cor Wolffs and Marcus Hemminga, University of Wageningen, are acknowledged for initial help with the sample preparation. This work was supported by BBSRC (43/B04750) and the EU (TMR contract no. FMRX-CT96-0004). C. Glaubitz was the recipient of a C. Rhodes Scholarship.

## References

[1] P.M.G.F. Van Wezenbeck, T.J.M. Hulsebos, J.G.G. Schoenmakers, Gene 11 (1980) 129–148.
[2] R. Bayer, G.W. Feigenson, Biochim. Biophys. Acta 815 (1985) 369–379.
[3] D.A. Marvin, E.J. Wachtel, Nature 253 (1975) 19–23.
[4] T.A. Cross, S.J. Opella, J. Mol. Biol. 182 (1985) 367–381.
[5] D.A. Marvin, Curr. Opin. Struct. Biol. 8 (1998) 150–158.
[6] Y. Nozaki, J. Reynolds, C. Tanford, Biochemistry 17 (1978) 1239–1246.
[7] K.P. Datema, A.J.W.G. Visser, A. Van Hoek, C.J.A.M. Wolfs, R.B. Spruijt, M.A. Hemminga, Biochemistry 26 (1987) 6145–6152.
[8] P.A. McDonnell, L. Shon, Y. Kim, S.J. Opella, J. Mol. Biol. 233 (1993) 447–463.
[9] M.A. Hemminga, J.C. Sanders, R.B. Spruijt, Prog. Lipid Res. 31 (1992) 301–333.
[10] R.B. Spruijt, M.A. Hemminga, Biochemistry 30 (1991) 11147–11154.
[11] J.D.J. O'Neil, B.D. Sykes, Biochemistry 27 (1988) 2753–2762.
[12] F.C.L. Almeida, S.J. Opella, J. Mol. Biol. 270 (1997) 481–495.
[13] G.D. Henry, J.H. Weiner, B.D. Sykes, Biochemistry 25 (1986) 590–598.
[14] C.H.M. Papavoine, M.L. Remerowski, L.M. Horstink, R.N.H. Konings, C.W. Hilbers, F.J.M. Van de Ven, Biochemistry 36 (1997) 4015–4026.
[15] D.P. Raleigh, M.H. Levitt, R.G. Griffin, Chem. Phys. Lett. 146 (1988) 71–76.
[16] A. Kubo, C.A. McDowell, J. Chem. Soc. - Faraday Trans. 84 (1988) 3713–3730.
[17] F. Creuzet, A. Mcdermott, R. Gebhard, K. Vanderhoef, M.B. Spijkerassink, J. Herzfeld, J. Lugtenburg, M.H. Levitt, R.G. Griffin, Science 251 (1991) 783–786.
[18] C. Glaubitz, A. Watts, J. Magn. Res. 130 (1998) 305–316.
[19] C. Glaubitz, I. Burnett, G. Groebner, J. Mason, A. Watts, J. Am. Chem. Soc. 121 (1999) 5787–5794.
[20] M. Maricq, J.S. Waugh, J. Chem. Phys. 70 (1979) 3300–3316.
[21] M. Mehring, Principles of High Resolution NMR in Solids, Springer Verlag, Berlin, 1983.
[22] K. Schmidt-Rohr, H.W. Spiess. Multidimensional Solid-State NMR and Polymers, Academic Press, London, 1994.
[23] R.B. Spruijt, J.A.M. Wolfs, M.A. Hemminga, Biochemistry 28 (1989) 9158–9165.
[24] D.R. Lide, CRC Handbook of Chemistry and Physics: A Ready-Reference Book of Chemical and Physical Data, CRC Press, Boca Raton, FL, 1997.
[25] P. Caravatti, G. Bodenhausen, R.R. Ernst, J. Magn. Res. 55 (1983) 88–103.
[26] M.H. Levitt, D.P. Raleigh, F. Creuzet, R.G. Griffin, J. Chem. Phys. 92 (1990) 6347–6364.
[27] C. Glaubitz, D. Phil Thesis, University of Oxford, Oxford, 1998.
[28] O.B. Peersen, M. Groesbeek, S. Aimoto, S.O. Smith, J. Am. Chem. Soc. 117 (1995) 7228–7237.
[29] J. Heller, R. Larsen, M. Ernst, A.C. Kolbert, M. Baldwin, S.B. Prusiner, D.E. Wemmer, A. Pines, Chem. Phys. Lett. 251 (1996) 223–229.
[30] R.G.S. Spencer, K.J. Halverson, M. Auger, A.E. McDermott, R.G. Griffin, P.T. Lansbury, Biochemistry 30 (1991) 10382–10387.
[31] C.J. Hartzell, M. Whitfield, T.G. Oas, G.P. Drobny, J. Am. Chem. Soc. 109 (1987) 5966–5969.
[32] R.E. Stark, L.W. Jelinski, D.J. Ruben, D.A. Torchia, R.G. Griffin, J. Magn. Res. 55 (1983) 266–273.
[33] K. Eichele, M.D. Lumsden, R.E. Wasylishen, J. Phys. Chem. 97 (1993) 8909–8916.
[34] A.E. Walling, R.E. Pargas, A.C. deDios, J. Phys. Chem. 101 (1997) 7299–7303.
[35] T.E. Creighton, Proteins: Structure and Molecular Properties, W.H. Freeman, New York, 1993.
[36] A.A. Nevzorov, S. Moltke, M.P. Heyn, M.F. Brown, J. Am. Chem. Soc. 121 (1999) 7636–7643.
[37] J. Herzfeld, A.E. Berger, J. Chem. Phys. 73 (1980) 6021.
[38] Q. Teng, T.A. Cross, J. Magn. Res. 85 (1989) 439–447.
[39] Q. Teng, M. Iqbal, T.A. Cross, J. Am. Chem. Soc. 114 (1992) 5312–5321.
[40] J.G. Hexem, M.H. Frey, S.J. Opella, J. Am. Chem. Soc. 103 (1981) 226–228.
[41] A.C. Olivieri, J. Magn. Res. 81 (1989) 201–205.
[42] J.C. Sanders, P.I. Haris, D. Chapman, C. Otto, M.A. Hemminga, Biochemistry 32 (1993) 12446–12454.
[43] K.A. Williams, C.M. Deber, Biochemistry 35 (1996) 10472–10483.

[44] A.R. Khan, K.A. Williams, J.M. Boggs, C.M. Deber, Biochemistry 34 (1995) 12388–12397.
[45] E. Thiaudiere, M. Soekarjo, E. Kuchinka, A. Kuhn, H. Vogel, Biochemistry 32 (1993) 12186–12196.
[46] F.M. Marassi, A. Ramamoorthy, S.J. Opella, Proc. Natl. Acad. Sci. USA 94 (1997) 8551–8556.
[47] J.U. Bowie, J. Mol. Biol. 272 (1997) 780–789.
[48] K.G. Valentine, D.M. Schneider, G.C. Leo, L.A. Colnago, S.J. Opella, Biophys. J. 49 (1986) 36–38.
[49] W.M. Tan, R. Jelinek, S.J. Opella, P. Malik, T.D. Terry, R.N. Perham, J. Mol. Biol. 286 (1999) 787–796.